APPLICATION OF MICROWAVE TECHNIQUES IN THE ANALYSIS OF QUANTUM WAVEGUIDE STRUCTURES AND DEVICES*

A. Weisshaar, J. Lary, S. M. Goodnick, and V. K. Tripathi

Department of Electrical and Computer Engineering

Oregon State University

Corvallis, OR 97331

ABSTRACT

An extension of the generalized scattering matrix (GSM) technique is formulated to compute the GSM of nonuniform quantum waveguide structures with two-dimensional quantum confinement of electronic states. Low temperature *I-V* characteristics for a double constriction are presented, exhibiting a region of negative differential resistance (NDR). A simple design procedure for increasing the temperature range with achievable NDR is introduced.

I. INTRODUCTION

The well developed numerical microwave techniques used in the analysis of guided-wave structures for microwave circuits (e.g.,1) are routinely applied to guided-wave configurations in other fields such as optical and acoustical waveguides. Over the past years, microwave techniques have also been increasingly applied to semiconductor structures as in (2) where simple transmission line techniques have been used to evaluate the properties of general semiconductor superlattices. Recently, a new class of semiconductor structures has emerged in which two-dimensional quantum confinement of electronic states is achieved (3). At low temperature, electronic transport in such quantum structures may be essentially ballistic so that the wave-like behavior of electrons dominates. Hence, the low-temperature electronic transport in these quantum waveguide structures is in close analogy to the propagation of electromagnetic waves in metallic waveguide circuits. However, unlike metallic waveguides, the sidewalls in quantum waveguides are defined by potential barriers which can be controlled by an externally applied voltage as shown in recent experiments on short split-gate field-effect transistors (4,5). There, conductance plateaus and oscillations (6) as a function of gate voltage have been observed. Theoretical calculations assuming a uniform quantum waveguide section with infinite potential walls (hard walls) which is connected to wide regions to model the coupling to the external system, correlate to this observed behavior (e.g.,7,8).

*This work was supported in part by the U.S. Office of Naval Research under Contract N00014-89-J-1894 and Tektronix, Inc., Beaverton, OR. J. L. acknowledges support from IBM Corp., Essex Junction, VT.

II. THEORETICAL FORMULATION

In this paper, an analysis procedure for nonuniform quantum waveguide structures which may be realized in the split-gate configuration is described. The nonuniform waveguide structure is first decomposed into uniform waveguide sections and junctions. In the present work, it is assumed that the electron motion in each uniform waveguide section is ballistic, and that the electronic states are governed by the time-independent Schrödinger equation in the effective mass approximation

$$\nabla^2\psi + \frac{2m^*}{\hbar^2}(E-V)\psi = \left(\nabla^2 + k_E^2 - k_V^2\right)\psi = 0 \qquad (1)$$

with lateral confinement by infinite potential walls (hard walls) (e.g.,3,8-11). Here, E represents the total electron energy, V the potential energy, m^* denotes the effective mass, and $\hbar$ is the reduced Planck's constant. Furthermore, the wavefunction ψ and its normal derivative are continuous across the interface between two uniform waveguide sections. The eigensolutions of (1) constitute the modes (energy subbands) of the uniform quantum waveguide. They form a complete infinite set of orthogonal functions, and hence, can be used as a modal expansion of the wavefunction in the uniform waveguide. For a uniform quantum waveguide of width w, the wavefunction is expanded into an infinite series of normal modes as

$$\psi = \sum_{m=1}^{\infty}\left(\psi_m^+ + \psi_m^-\right) = \sum_{m=1}^{\infty}\left(a_m e^{i\beta_m z} + b_m e^{-i\beta_m z}\right)\sqrt{Z_m}\,\phi_m(x) \qquad (2a)$$

$$\text{with} \quad \beta_m = \sqrt{k_E^2 - k_V^2 - k_c^2(m)}\,, \quad k_c(m) = \frac{m\pi}{w} \qquad (2b)$$

$$\text{and} \quad \phi_m(x) = \sqrt{2/w}\,\sin\left[k_c(m)x\right] \qquad (2c)$$

and properly truncated for numerical solutions. The quantity Z_m is defined as the ratio of ψ_m^+ and $-i\partial\psi_m^+/\partial z$, and represents the generalized characteristic wave impedance for modal waves propagating in the positive z-direction.

Mode-matching methods (1,8,12) are then employed to compute the generalized scattering matrices (GSM's) (1) of the junctions. The GSM of the composite quantum waveguide structure may be obtained by combining the generalized scattering parameters of the junctions and the uniform waveguide section via the GSM technique (1). In the GSM

technique, however, the same number of modes are retained in the waveguide section and in the two junctions it connects. For an accurate computation of the GSM of a junction, a significant number of evanescent modes may need to be included, although most of these modes do not couple effectively to the next junction due to the large attenuation of their amplitudes. Therefore, either highly attenuated evanescent modes may need to be included for an accurate characterization of the junctions leading to numerical instabilities in form of ill-conditioned matrices, or the number of evanescent modes is limited to only those that are effectively coupled between the two junctions, thus impairing the accuracy of the scattering parameters of the junctions. These drawbacks are eliminated in the extended GSM technique introduced below where the number of modes retained in the waveguide section and the two junctions may be different. Consequently, the GSM's of the junctions can be determined to any desired accuracy while assuring a numerically stable GSM for the composite structure.

Figure 1 shows the configuration of two arbitrary junctions (A and B) which are connected through a uniform waveguide section (C). The modal amplitudes are expressed by the column vectors $\boldsymbol{a}_a^A$, $\boldsymbol{b}_a^A$ etc. The total number of modes retained on each side of the junctions is grouped into the number of modes K coupled between A and B, and the remaining modes as indicated in Fig. 1.

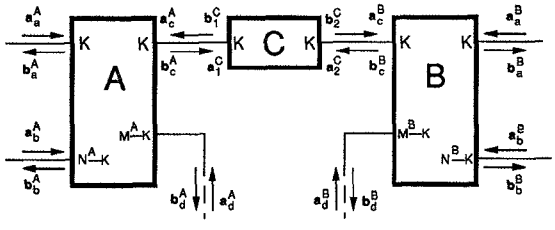

Fig. 1: Two arbitrary junctions (A and B) connected by a uniform waveguide section (C).

In terms of the GSM of junction A, this partitioning rule is expressed as

$$\begin{bmatrix} \boldsymbol{b}_1^A \\ \boldsymbol{b}_2^A \end{bmatrix} = \begin{bmatrix} \boldsymbol{b}_a^A \\ \boldsymbol{b}_b^A \\ \boldsymbol{b}_c^A \\ \boldsymbol{b}_d^A \end{bmatrix} = \begin{bmatrix} \boldsymbol{S}_{aa}^A & \boldsymbol{S}_{ab}^A & \boldsymbol{S}_{ac}^A & \boldsymbol{S}_{ad}^A \\ \boldsymbol{S}_{ba}^A & \boldsymbol{S}_{bb}^A & \boldsymbol{S}_{bc}^A & \boldsymbol{S}_{bd}^A \\ \boldsymbol{S}_{ca}^A & \boldsymbol{S}_{cb}^A & \boldsymbol{S}_{cc}^A & \boldsymbol{S}_{cd}^A \\ \boldsymbol{S}_{da}^A & \boldsymbol{S}_{db}^A & \boldsymbol{S}_{dc}^A & \boldsymbol{S}_{dd}^A \end{bmatrix} \begin{bmatrix} \boldsymbol{a}_a^A \\ \boldsymbol{a}_b^A \\ \boldsymbol{a}_c^A \\ \boldsymbol{a}_d^A \end{bmatrix} = \begin{bmatrix} \boldsymbol{S}_{11}^A & \boldsymbol{S}_{12}^A \\ \boldsymbol{S}_{21}^A & \boldsymbol{S}_{22}^A \end{bmatrix} \begin{bmatrix} \boldsymbol{a}_1^A \\ \boldsymbol{a}_2^A \end{bmatrix} \tag{3}$$

A corresponding partitioned GSM is obtained for junction B and is given by (3) with superscript A replaced by B. The uniform waveguide section C of length L can be characterized by the diagonal matrix $\boldsymbol{P}$ with diagonal elements

$$P(m,m) = e^{i\beta_m^C L}, \quad m = 1,2,3,\ldots,K. \tag{4}$$

To obtain the GSM of the composite structure, the boundary conditions for the amplitudes at the interfaces between A and C as well as B and C (Fig. 1) are imposed while the incident amplitudes for the uncoupled evanescent modes are set to zero. After eliminating the mode amplitudes of the uniform waveguide section, the generalized scattering parameters of the composite structure with amplitude vectors defined as

$$\boldsymbol{a}_1 = \begin{bmatrix} \boldsymbol{a}_a^A \\ \boldsymbol{a}_b^A \end{bmatrix} \quad \boldsymbol{b}_1 = \begin{bmatrix} \boldsymbol{b}_a^A \\ \boldsymbol{b}_b^A \end{bmatrix} \quad \boldsymbol{a}_2 = \begin{bmatrix} \boldsymbol{a}_a^B \\ \boldsymbol{a}_b^B \end{bmatrix} \quad \boldsymbol{b}_2 = \begin{bmatrix} \boldsymbol{b}_a^B \\ \boldsymbol{b}_b^B \end{bmatrix} \tag{5}$$

are obtained as

$$\boldsymbol{S}_{11} = \begin{bmatrix} \boldsymbol{S}_{aa}^A & \boldsymbol{S}_{ab}^A \\ \boldsymbol{S}_{ba}^A & \boldsymbol{S}_{bb}^A \end{bmatrix} + \begin{bmatrix} \boldsymbol{S}_{ac}^A \boldsymbol{P}\left(\boldsymbol{I} - \boldsymbol{S}_{cc}^B \boldsymbol{P} \boldsymbol{S}_{cc}^A \boldsymbol{P}\right)^{-1} \boldsymbol{S}_{cc}^B \boldsymbol{P} \begin{bmatrix} \boldsymbol{S}_{ca}^A & \boldsymbol{S}_{cb}^A \end{bmatrix} \\ \boldsymbol{S}_{bc}^A \boldsymbol{P}\left(\boldsymbol{I} - \boldsymbol{S}_{cc}^B \boldsymbol{P} \boldsymbol{S}_{cc}^A \boldsymbol{P}\right)^{-1} \boldsymbol{S}_{cc}^B \boldsymbol{P} \begin{bmatrix} \boldsymbol{S}_{ca}^A & \boldsymbol{S}_{cb}^A \end{bmatrix} \end{bmatrix} \tag{6a}$$

$$\boldsymbol{S}_{12} = \begin{bmatrix} \boldsymbol{S}_{ac}^A \boldsymbol{P}\left(\boldsymbol{I} - \boldsymbol{S}_{cc}^B \boldsymbol{P} \boldsymbol{S}_{cc}^A \boldsymbol{P}\right)^{-1} \begin{bmatrix} \boldsymbol{S}_{ca}^B & \boldsymbol{S}_{cb}^B \end{bmatrix} \\ \boldsymbol{S}_{bc}^A \boldsymbol{P}\left(\boldsymbol{I} - \boldsymbol{S}_{cc}^B \boldsymbol{P} \boldsymbol{S}_{cc}^A \boldsymbol{P}\right)^{-1} \begin{bmatrix} \boldsymbol{S}_{ca}^B & \boldsymbol{S}_{cb}^B \end{bmatrix} \end{bmatrix} \tag{6b}$$

as well as $\boldsymbol{S}_{21}$ and $\boldsymbol{S}_{22}$ which are given by (6b) and (6a), respectively, with superscripts A and B interchanged.

From the scattering parameters of the composite structure, the total transmission coefficient T_n from propagating mode n at the input to all M_p propagating modes at the output is found as

$$T_n = \sum_{m=1}^{M_p} \left| S_{21}(m,n) \right|^2 \tag{7}$$

The total transmission T through a quantum waveguide structure can be defined as the summation of T_n over all propagating modes at the input. For small bias voltages (linear response regime), the total transmission evaluated at the Fermi energy E_f is equivalent to the normalized zero-temperature conductance (7). A more general expression for the current through a quantum waveguide structure as a function of applied bias voltage V_b is given as (13)

$$I(V_b) = \frac{2e}{h} \int_0^\infty \left[f(E) - f(E+eV_b) \right] T(E,V_b)\, dE \tag{8}$$

where $f(E)$ is the carrier distribution function, here assumed to be a Fermi-Dirac function. Here, the effect of an applied bias voltage is modeled as linear potential drops across the uniform waveguide sections. In the numerical analysis, a stepped guide model is used to approximate each linear potential drop.

III. COMPUTATIONAL RESULTS

The modal analysis method described above has been applied to various nonuniform quantum waveguide structures which may be realized in a split-gate GaAs/AlGaAs heterojunction configuration. Among them are single and double bend structures (8) and the double constriction. The case of the double constriction shown in the inset of Fig. 2(a) is of special interest due to the analogy to evanescent mode filters and to the resonant tunneling diode (RTD) which is finding applications at millimeter and microwave frequencies. The total transmission coefficient T for a biased double constriction exhibits sharp resonant peaks similar to RTD's (14) at energies for which no waves can propagate in the two narrow constrictions (Fig. 2(a)). The calculated I-V characteristics shown in Fig. 2(b) for various temperatures exhibit a region of negative differential resistance (NDR).

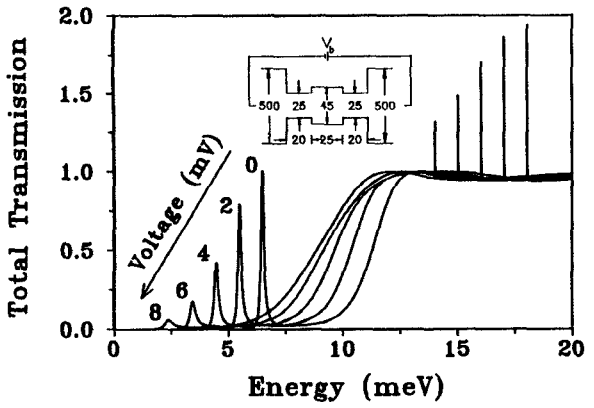

(a)

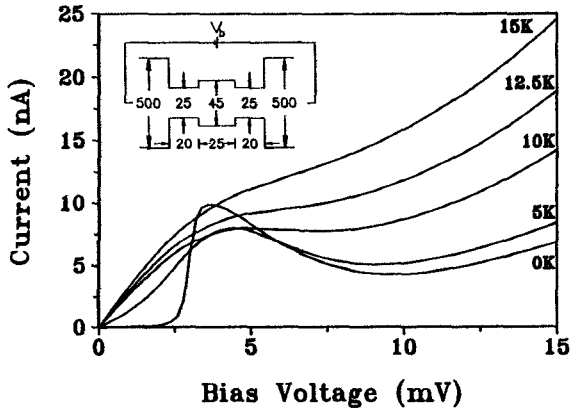

(b)

Fig. 2: (a) Total transmission T as function of energy and different values of bias voltage for the double constriction structure shown in the inset (dimensions are in nm); (b) I-V characteristics at different temperatures for the double constriction structure shown in the inset; E_f=5meV.

A simple design procedure for symmetric double constriction structures has been developed to enhance the temperature range with achievable NDR. If only the lowest-order mode in the cavity region is considered, an expression for the total transmission through a symmetric double constriction at zero bias voltage, similar to that for a one-dimensional double potential barrier (15), can be found as

$$T(E) = \left(1 + \frac{4R_b}{T_b^2}\sin^2(\beta L + \varphi)\right)^{-1} \qquad (9)$$

where $T_b = 1\text{-}R_b$ is the total transmission through a single narrow constriction (barrier). The quantity φ is the phase factor of the reflection coefficient for electrons in the cavity facing the left or right narrow constriction. It can be accurately approximated by the phase ϕ of the reflection coefficient for a single step discontinuity at the interfaces of the cavity and the two narrow constrictions (Fig. 3).

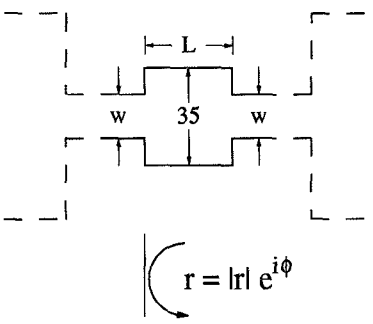

Fig. 3: Reflection coefficient r for the step discontinuity from the cavity region to the narrow constrictions.

The resonance energy for which T=1 is given by the resonance condition $\beta L + \varphi = n\pi$ (n=0,1,2,···), and can be determined graphically as shown in Fig. 4. There, βL and $-\phi$ (to approximate $-\varphi$) are plotted as a function of energy for various lengths L of the cavity and widths w of the two narrow constrictions. Also evident in the figure is the cutoff energy of the lowest-order mode in the two narrow constrictions as indicated by the sharp discontinuities in the ($-\phi$) curves.

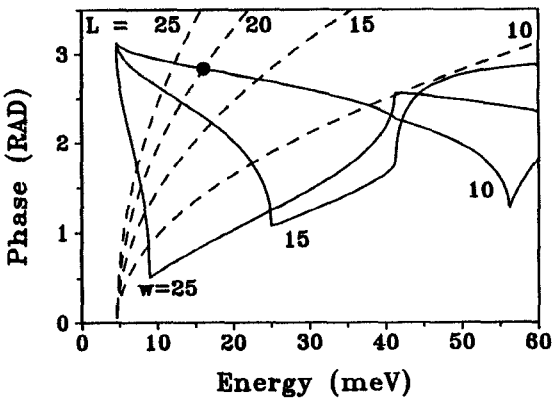

Fig. 4: Phase $-\phi = -\arg(r)$ (solid lines) and phase shift βL (dashed lines) inside the cavity region.

In order to increase the temperature range with achievable NDR, a large energy gap between the lowest-order resonance and the cutoff energy in the narrow constriction as well as the second-lowest resonance is needed. The length of the two narrow constrictions has very little influence on the position of the resonance, however, it controls the width of the resonant peak through T_b (the width of the peak decreases with increasing length of the narrow constrictions). As a compromise between a practical size of the width of the resonance peak (large current) and a large temperature range with achievable NDR, new dimensions for the double constriction structure were chosen as indicated in Fig. 4 and in the inset of Fig. 5. The predicted resonance energy (16.02meV) is found to be very close to the actual resonance (15.98meV) obtained from the transmission data. The corresponding I-V curves with enhanced temperature range with achievable NDR are shown in Fig. 5.

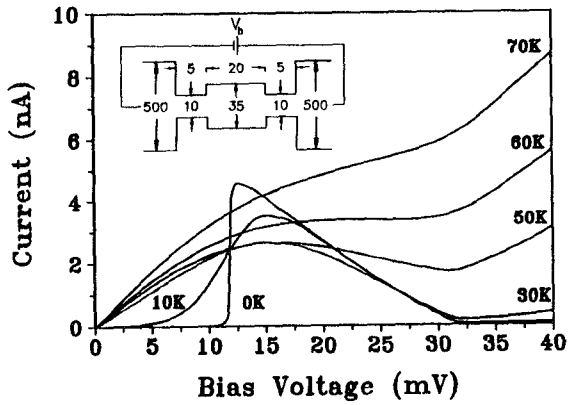

Fig. 5: I-V characteristics at different temperatures for the improved structure shown in the inset; E_f=10meV (dimensions are in nm).

It is obvious from Figs. (2a,b) that the total transmission evaluated at the current peak may be considerably less than unity. In order to maximizes the total transmission near the current peak, the simple design procedure for symmetric double constrictions presented above has been extended to asymmetric double constriction structures with different lengths of the left and right narrow constriction. Results for the I-V characteristics, however, indicate that an increased temperature range with achievable NDR is not necessarily obtained.

IV. SUMMARY

An extension of the generalized scattering matrix technique to decouple some of the evanescent modes has been described. The method has been applied to analyze non-uniform quantum waveguide structures. The calculated *I-V* characteristics for a double constriction structure exhibit a region of NDR at low temperature. A simple design procedure to enhance the temperature range with achievable NDR has been presented. The method described here should be useful in the analysis of other non-uniform quantum waveguide structures exhibiting new quantum interference effects, as well as to guided-wave structures in microwave integrated circuits (MIC's) and optical integrated circuits (OIC's).

REFERENCES

(1) T. Itoh, Ed., *Numerical Techniques for Microwave and Millimeter-Wave Passive Structures*, New York: Wiley, 1989.

(2) V. K. Tripathi and P. K. Bhattacharya, "Electron energy states and miniband parameters in a class of non-uniform quantum well superlattice structures," *Superlattices and Microstructures*, vol. 1 pp. 73-79, 1985.

(3) M. A. Reed and W. P. Kirk, Eds., *Nanostructure Physics and Fabrication*, Boston: Academic, 1989.

(4) B. J. Van Wees *et al.*, "Quantized conductance of point contacts in a two-dimensional electron gas," *Phys. Rev. Lett.*, vol. 60, pp. 848-850, 1988.

(5) D. A. Wharam *et al.*, "One-dimensional transport and the quantisation of the ballistic resistance," *J. Phys. C: Solid State Phys.*, vol. 21, pp. L209-L214, 1988.

(6) R. J. Brown *et al.*, "The one dimensional quantised ballistic resistance in GaAs/AlGaAs heterojunctions with varying experimental conditions," *Solid-State Electron.*, vol. 32, pp. 1179-1183, 1989.

(7) A. Szafer and A. D. Stone, "Theory of quantum conduction through a constriction," *Phys. Rev. Lett.*, vol. 62, pp. 300-303, 1989.

(8) A. Weisshaar *et al.*, "Analysis of discontinuities in quantum waveguide structures," *Appl. Phys. Lett.*, vol. 55, pp. 2114-2116, 1989.

(9) F. Sols *et al.*, "On the possibility of transistor action based on quantum interference phenomena," *Appl. Phys. Lett.*, vol. 54, pp. 350-352, 1989.

(10) C. S. Lent, S. Sivaprakasam, and D. J. Kirkner, "A two-dimensional hot carrier injector for electron waveguide structures," *Solid-State Electron.*, vol 54, pp. 1137-1141, 1989.

(11) A. Weisshaar *et al.*, "Negative differential resistance in a resonant quantum wire structure," *Electron Device Lett.*, EDL-12, Jan. 1991.

(12) E. Kühn, "A mode-matching method for solving field problems in waveguide and resonator circuits," *Arch. Elek. Übertragung.*, vol. 27, pp. 511-513, 1973.

(13) S. Datta, "Quantum devices," *Superlattices and Microstructures*, vol. 6, pp. 83-93, 1989.

(14) F. Capasso, K. Mohammed, and A. Y. Cho, "Resonant tunneling through double barriers, perpendicular quantum transport phenomena in superlattices, and their device applications," *IEEE J. Quantum Electron.*, QE-22, 1853-1868, 1986.

(15) S. Datta, *Quantum Phenomena*, Modular series on solid state devices, vol. VIII, edited by F. Pierret and G. W. Neudeck, Reading: Addison-Wesley, 1989.